

Searching for missing direct photons in heavy-ion collisions with P and CP violation

Jonathan D. Kroth^{1,*} and Kirill Tuchin^{1,†}

¹*Department of Physics and Astronomy, Iowa State University, Ames, Iowa 50011, USA*

(Dated: February 4, 2026)

We compute synchrotron radiation from a plasma in which P - and CP -violating parameters, a chiral chemical potential and a chiral gradient, couple to fermions. To do this, we compute exact wavefunctions for the fermions in the presence of these parameters and an external constant magnetic field. We find that these parameters increase the synchrotron radiation emitted by the fermions while also decreasing the traditionally large synchrotron radiation elliptic flow coefficient v_2 . We apply these results to the quark-gluon plasma, where just such a contribution could provide a solution to the missing direct photons puzzle. We also use our wavefunctions to give a derivation of the chiral magnetic effect.

I. INTRODUCTION

The traditional mechanism of direct photon production in relativistic heavy-ion collisions relies on conventional perturbation theory to describe short-distance processes and hydrodynamic approximation to account for the collective behavior of the quark-gluon plasma (QGP). This approach has proven fairly successful in providing a phenomenological framework [1–19]. However, it faces challenges in simultaneously describing the soft part of the photon spectrum and its variation with the azimuthal angle around the collision axis. This is because it either predicts an insufficient number of photons or too mild variation with the azimuthal angle, as quantified by the elliptic flow.

Several solutions have been proposed to solve this problem [20–32]. Among these, one of the most promising approaches involves incorporating the synchrotron photons emitted by the QGP due to the presence of a strong magnetic field. This synchrotron radiation not only provides additional photons, but also exhibits a highly anisotropic distribution. As a result, it significantly enhances the elliptic flow, as most of the synchrotron radiation is emitted perpendicular to the magnetic field. In fact, the elliptic flow of photons generated by the strong magnetic field exceeds

* jkroth@iastate.edu

† tuchink@gmail.com

the experimental data. The situation is further complicated in the presence of rotation, which tends to amplify the effect of the magnetic field, as we have recently demonstrated in [31–34].

In this paper, we argue that the elliptic flow v_2 strongly depends on the chiral properties of the QGP. Specifically, it depends on the transport coefficients associated with the chiral magnetic and anomalous Hall currents. These currents are directly associated with the chiral anomaly and, as such, violate P and CP -symmetries. In particular, we find that non-zero values for either of these parameters significantly reduces v_2 . The reason that the chiral magnetic current reduces the elliptic flow may be that the current flows in the direction of the magnetic field and the relativistic quarks emit photons mostly in the forward direction. In contrast, synchrotron radiation is emitted mostly perpendicular to the magnetic field. A different mechanism of photon production via the chiral anomaly in the presence of a magnetic field, but ignoring synchrotron radiation, was previously considered in [24, 25, 27, 35–38].

Our objective is to develop a consistent theoretical framework for computing photon radiation in the presence of anomalous currents. A powerful approach to accomplish this goal is to employ an effective field theory which adds to the standard electromagnetic interaction the following term [39–43]:

$$\mathcal{L}_{\text{anom}} = \partial_\mu \theta j^{\mu 5} = b_\mu j^{\mu 5}, \quad (1)$$

which couples the chiral vector current $j^{\mu 5} = \bar{\psi} \gamma^\mu \gamma^5 \psi$ to the background pseudoscalar field θ . The equations of motion depend on the vector field $b_\mu = \partial_\mu \theta$,¹ whose time component has the physical meaning of a chiral chemical potential μ_5 , while the spatial components are most familiar as the displacement in momentum space of the Weyl nodes of a semimetal. The anomalous currents associated with b_μ are the chiral magnetic current $\mathbf{j} = c_A b_0 \mathbf{B}$ and the anomalous Hall current $\mathbf{j} = c_A \mathbf{b} \times \mathbf{E}$. Throughout this paper, b_μ is assumed to be constant.

Alternatively, the same physics can be described by coupling the field invariant $F_{\mu\nu} \tilde{F}^{\mu\nu}$ to θ . We have pursued this method in our previous publications [36, 50–52]. The two effective theories are related to each other in the chiral limit by a chiral transformation. Therefore, while each approach offers a different vantage point, in the chiral limit, the final results must remain independent of the choice of the effective theory. However, establishing such equivalence in practice may be challenging.

This paper employs the approach based on the effective term given by Eq. (1). The resulting equation of motion, including coupling to a background magnetic field, is given by Eq. (2). Our

¹ In this paper it is convenient to define $b_\mu = \partial_\mu \theta$, consistent with [39, 40, 44]. Another definition $b_\mu = c_A \partial_\mu \theta$ is also often used in the literature, e.g. [28, 45–49].

goal is to solve this equation and utilize its solutions to investigate the photon production by the QGP.

Recently, Shovkovy and Wang conducted a similar calculation [53]. They employed a relationship between the photon production rate and the fermion propagator in a magnetic field at a finite chiral chemical potential μ_5 , which is identified with b_0 . Unlike [53], we do not restrict ourselves to the chiral limit and also take into account b_3 , associated with the longitudinal component of the anomalous Hall current.

The paper is structured as follows: in Section II, we derive solutions to the modified Dirac equation given by (2) in a constant magnetic field. These spinors, expressed by (36), constitute our main theoretical result. We turn to phenomenology in Section III, where we use these spinors to compute the synchrotron radiation emitted by these fermions. We complete this calculation numerically in Section IV. We conclude in Section V. As another application of our wavefunctions, we compute the chiral magnetic current using them in Appendix A.

We employ the natural units $\hbar = c = k_B = 1$ and use the following notations: $p^\mu = (E, \mathbf{p})$, $k^\mu = (\omega, \mathbf{k})$, $b^\mu = (b_0, \mathbf{b})$, with $b_0 = \mu_5$ being the chiral chemical potential. We refer to \mathbf{b} as the chiral gradient.

II. DIRAC EQUATION WITH CHIRAL COUPLINGS

We wish to solve the Dirac equation

$$(i\mathcal{D} - \gamma^5 \not{b} - m)\psi = 0, \quad (2)$$

where D is the covariant derivative, for a particle of charge q and mass m in the presence of a constant magnetic field \mathbf{B} which points along the 3-axis. The field b_μ is assumed to be constant, with only two non-vanishing components: b_0 and b_3 .

We use the general gauge choice

$$A_\mu = (0, aBy, -(1-a)Bx, 0) \quad (3)$$

with $a \in [0, 1]$. $a = \frac{1}{2}$ corresponds to the symmetric Landau gauge, which we will use explicitly later when it becomes useful to choose a gauge.

A. Determination of Two-Component Spinors

To solve Eq. (2), we write

$$\psi(x) = e^{-iEt+ip_3z} \begin{pmatrix} \chi_-(\mathbf{x}_\perp) \\ \chi_+(\mathbf{x}_\perp) \end{pmatrix}. \quad (4)$$

with χ_σ two-component spinors. Throughout this paper, we allow E to be negative. We use $\sigma = \pm 1$ throughout this paper to denote chirality. In the Weyl representation, the Dirac equation (2) gives

$$\begin{pmatrix} E - b_3 - \sigma(p_3 - b_0) & \sigma D_-^\perp \\ \sigma D_+^\perp & E + b_3 + \sigma(p_3 + b_0) \end{pmatrix} =: \Pi_\sigma \chi_\sigma = m \chi_{-\sigma} \quad (5)$$

Note as well that $b_3 = \mathbf{b} \cdot \hat{z}$ is the spatial component of b^μ . We have defined, for $\tau = \pm 1$,

$$D_\tau^\perp = (iD_1 - \tau D_2). \quad (6)$$

We can decouple these first-order equations by making them second order:

$$\begin{pmatrix} (E - b_3)^2 - (p_3 - b_0)^2 - D_-^\perp D_+^\perp & -2D_-^\perp(b_0 + \sigma b_3) \\ -2D_+^\perp(b_0 - \sigma b_3) & (E + b_3)^2 - (p_3 + b_0)^2 - D_+^\perp D_-^\perp \end{pmatrix} \chi_\sigma = \Pi_{-\sigma} \Pi_\sigma \chi_\sigma = m^2 \chi_\sigma. \quad (7)$$

Now, it is known that when $b_0 = b_3 = 0$, the eigenfunctions $\psi(x)$ are simple harmonic oscillator wavefunctions; in that case, the operators D_\pm^\perp serve as the raising and lowering operators. Since $\not{p} \gamma^5$ commutes with \not{D}^\perp , these simple harmonic oscillator states will continue to be useful as spatial eigenfunctions. Notice that, had we allowed b_1 or b_2 to be non-zero (equivalent by a change of coordinates and a gauge transformation), this would not be the case, and our analysis would be much more difficult.

To this end, choose an orthonormal basis $\{\phi_n(\mathbf{x}_\perp)\}_n$ of spinor simple harmonic oscillator eigenfunctions appropriate to the choice of gauge.² A straightforward calculation shows

$$D_\tau^\perp \phi_n = -\sqrt{2|qB|} \left(n + \frac{1 - \tau\beta}{2} \right) \phi_{n-\tau\beta}, \quad D_\tau^\perp D_{-\tau}^\perp \phi_n = 2|qB| \left(n + \frac{1 + \tau\beta}{2} \right) \phi_n, \quad (8)$$

where $\beta = \text{sgn}(qB)$. Write $\chi_{\beta\sigma}$ in terms of these eigenfunctions,

$$\chi_{\beta\sigma} = \sum_{n=0}^{\infty} \begin{pmatrix} c_n^{\beta\sigma} \phi_n \\ d_n^{\beta\sigma} \phi_n \end{pmatrix}, \quad (9)$$

² The eigenfunctions ϕ_n are two-component spinors with two indices, n and another appropriate to the gauge choice.

For $a = \frac{1}{2}$, it is the azimuthal angular momentum j , while for $a = 1$, it is p_1 . We treat these additional points in Appendix B, as they do not affect the derivation of the wavefunctions.

where we have introduced a β subscript due to its appearance in Eq. (8). Using the orthonormality of the ϕ_n , one finds

$$0 = \begin{pmatrix} E^2 - \Lambda_n^2 - 2X & 2(b_0 + \sigma b_3) \sqrt{2|qB|n} \\ 2(b_0 - \sigma b_3) \sqrt{2|qB|n} & E^2 - \Lambda_n^2 + 2X \end{pmatrix} \begin{pmatrix} c_n^\sigma \\ d_n^\sigma \end{pmatrix}, \quad (10)$$

where we have defined

$$\Lambda_n^2 = p_3^2 + 2n|qB| + b^2 + m^2 \quad \text{and} \quad X = Eb_3 - p_3 b_0. \quad (11)$$

We have removed the index β by defining $c_n^\sigma = c_n^{+\sigma} = c_{n-1}^{-\sigma}$ and $d_n^\sigma = d_{n-1}^{+\sigma} = d_n^{-\sigma}$, for $n > 0$. That is, the equations determining $c_n^{\beta\sigma}$ and $d_n^{\beta\sigma}$ decouple into pairs of equations for $c_n^{\beta\sigma}$ and $d_{n-\beta}^{\beta\sigma}$. Had we allowed b_1 or b_2 to be non-zero, this would not have occurred — this is the difficulty mentioned above — and signals that a different spatial basis should be used. So there are eigenspinors

$$\chi_{\beta\sigma}^{(n)} = \begin{pmatrix} c_n^\sigma \phi_{n-}(\frac{1-\beta}{2}) \\ d_n^\sigma \phi_{n-}(\frac{1+\beta}{2}) \end{pmatrix} \quad (12)$$

It then remains to solve Eq. (10) for $n > 0$ and to analyze the special case of $n = 0$.

1. $n = 0$

In the case $n = 0$, we retain the additional index β . The same analysis leading to Eq. (10) leads to

$$(E^2 - \Lambda_0^2 - 2X)c_0^{+\sigma} = 0 \quad (13)$$

$$(E^2 - \Lambda_0^2 + 2X)d_0^{-\sigma} = 0. \quad (14)$$

All other terms trivially vanish since $c_{-1}^{\beta\sigma} = d_{-1}^{\beta\sigma} = 0$, by definition. Then, for a non-vanishing $n = 0$ spinor, $c_0^{+\sigma} = d_0^{-\sigma} = 1$, and we get the dispersion

$$(E - \beta b_3)^2 - (p - \beta b_0)^2 - m^2 = 0. \quad (15)$$

The $n = 0$ spinor is then

$$\chi_{\beta\sigma}^{(0)} = \begin{pmatrix} \frac{1+\beta}{2} \\ \frac{1-\beta}{2} \end{pmatrix} \phi_0. \quad (16)$$

2. $n > 0$

For $n \geq 1$, Eq. (10) gives the dispersion relation

$$(E^2 - \Lambda_n^2 - 2X)(E^2 - \Lambda_n^2 + 2X) = (E^2 - \Lambda_n^2)^2 - 4X^2 = 4b^2 2n|qB|. \quad (17)$$

This is a quartic in E whose solution cannot be succinctly written. For later use, we write this in another form,

$$((\tilde{p} + b)^2 - m^2)((\tilde{p} - b)^2 - m^2) = -4b^2 m^2, \quad (18)$$

with the shorthand $\tilde{p}^\mu = (E, 0, \sqrt{2n|qB|}, p_3)$.

Solving Eq. (10) and normalizing $\chi_{\beta\sigma}^{(n)}$ gives

$$|c_n^\sigma|^2 = \frac{1}{2} \frac{(b_0 + \sigma b_3)(E^2 - \Lambda_n^2 + 2X)}{b_0(E^2 - \Lambda_n^2) + 2\sigma b_3 X}, \quad (19)$$

$$|d_n^\sigma|^2 = \frac{1}{2} \frac{(b_0 - \sigma b_3)(E^2 - \Lambda_n^2 - 2X)}{b_0(E^2 - \Lambda_n^2) + 2\sigma b_3 X}. \quad (20)$$

Appealing to Eq. (10) again, we find the relative sign between c_n^σ and d_n^σ to be

$$s^\sigma := -\text{sgn} \left(\frac{E^2 - \Lambda_n^2 - 2\tau X}{b_0 + \sigma \tau b_3} \right), \quad (21)$$

for either choice of $\tau = \pm 1$. We will insert this sign by hand by choosing c_n^σ and d_n^σ to be positive and putting s^σ in the second component of $\chi_{\beta\sigma}^{(n)}$, i.e.

$$\chi_{\beta\sigma}^{(n)} = \begin{pmatrix} c_n^\sigma \phi_{n+\bar{\beta}} \\ s^\sigma d_n^\sigma \phi_{n+-\bar{\beta}} \end{pmatrix}. \quad (22)$$

The two signs are also related:

$$s^\sigma = -\text{sgn}(b^2) \text{sgn} \left(\frac{E^2 - \Lambda_n^2 - 2X}{b_0 - \sigma b_3} \right) = \text{sgn}(b^2) s^{-\sigma}. \quad (23)$$

Notice that s^σ is not well-defined in the limit $b_0, b_3 \rightarrow 0$. In that limit, the matrix equation for the two-component spinors becomes diagonal, signaling that we require more constraints to specify c_n^σ and d_n^σ uniquely. This is usually done by also requiring ψ to be an eigenspinor of a spin-like operator.

B. Determination of Dirac spinors

Now we will glue together the $\chi_{\beta\sigma}^{(n)}$ to form solutions to the Dirac equation. Write

$$\psi_\beta^{(n)} = \begin{pmatrix} f_n^\beta \chi_{\beta-}^{(n)} \\ g_n^\beta \chi_{\beta+}^{(n)} \end{pmatrix}. \quad (24)$$

The Dirac equation then gives an equation for the coefficients,

$$\begin{pmatrix} E - b_3 - \sigma(p_3 - b_0) & -\sigma\sqrt{2n|qB|} \\ -\sigma\sqrt{2n|qB|} & E + b_3 + \sigma(p_3 + b_0) \end{pmatrix} \begin{pmatrix} c_n^\sigma \\ d_n^\sigma \end{pmatrix} = m \left(\frac{f_n^\beta}{g_n^\beta} \right)^\sigma \begin{pmatrix} c_n^{-\sigma} \\ d_n^{-\sigma} \end{pmatrix} \quad (25)$$

where on the right-hand side σ is an exponent on the fraction rather than a label. At this point, it is evident that f_n^β and g_n^β do not depend on β for $n > 0$, so we will drop the associated superscripts.

1. $n = 0$

We first handle the $n = 0$ case. Since one of $c_0^{\beta\sigma}$ and $d_0^{\beta\sigma}$ is 0, we get one equation to solve,

$$\left(\frac{f_0^\beta}{g_0^\beta} \right)^\sigma = \frac{E - \beta b_3 - \beta\sigma(p_3 - \beta b_0)}{m}. \quad (26)$$

Normalizing the spinor gives

$$|f_0^\beta|^2 = \frac{E - \beta b_3 - \beta(p_3 - \beta b_0)}{2(E - \beta b_3)}, \quad (27)$$

$$|g_0^\beta|^2 = \frac{E - \beta b_3 + \beta(p_3 - \beta b_0)}{2(E - \beta b_3)}. \quad (28)$$

An analysis of the $n = 0$ dispersion relation shows that

$$\operatorname{sgn} \left(\frac{f_0^\beta}{g_0^\beta} \right) = \operatorname{sgn}(E - \beta b_3). \quad (29)$$

We choose to define f_0^β, g_0^β as positive and place this relative sign in the first two components.

2. $n > 0$

For $n > 0$, we can use the explicit forms of c_n^σ and d_n^σ as well as the dispersion relation to find

$$\left(\frac{f_n}{g_n} \right)^\sigma = \frac{\sigma \operatorname{sgn}(b_0 + \sigma b_3)}{2m} ((\tilde{p} + \sigma b)^2 - m^2) \sqrt{\frac{1}{b^2} \frac{b_0(E^2 - \Lambda_n^2) - 2\sigma b_3 X}{b_0(E^2 - \Lambda_n^2) + 2\sigma b_3 X}}, \quad (30)$$

where again $\tilde{p}^\mu = (E, 0, \sqrt{2n|qB|}, p_3)$. Normalizing $\psi_\beta^{(n)}$ gives

$$|f_n|^2 = \frac{((\tilde{p} + b)^2 - m^2)(b_0(E^2 - \Lambda_n^2) - 2b_3 X)}{4b^2(E(E^2 - \Lambda_n^2) - 2b_3 X)}, \quad (31)$$

$$|g_n|^2 = -\frac{((\tilde{p} - b)^2 - m^2)(b_0(E^2 - \Lambda_n^2) + 2b_3 X)}{4b^2(E(E^2 - \Lambda_n^2) - 2b_3 X)}. \quad (32)$$

The minus sign in $|g_n|^2$ may seem alarming, but recall the second form of the dispersion given by Eq. (18). The relative sign between f_n and g_n is

$$u := \operatorname{sgn} \left(\frac{f_n}{g_n} \right) = \operatorname{sgn} \left(\frac{(\tilde{p} + \sigma b)^2 - m^2}{b_0 + \sigma b_3} \right) \quad (33)$$

for either choice of σ . As for the $n = 0$ case, we insert this factor by hand in the first two components.

3. Summary of Dirac Spinors

Looking at Eqs. (19), (20), (31), and (32), there is a simplification that can be made: namely, the denominators of c_n^σ and d_n^σ can be canceled with part of the numerators of f_n and g_n . At the same time, we can consolidate our notation. Define, for $n > 0$,

$$C_{\sigma\tau} = \sqrt{\frac{-s^\sigma}{2} \frac{E^2 - \Lambda^2 + 2\tau X}{b_0 - \sigma\tau b_3}}, \quad (34)$$

$$G_\sigma = \sqrt{\frac{\sigma s^\sigma}{4} \frac{(\tilde{p} - \sigma b)^2 - m^2}{E(E^2 - \Lambda^2) - 2b_3 X}}. \quad (35)$$

These depend on n , but we suppress this index for brevity; for our applications there should be no confusion. The signs $-s^\sigma$ and σs^σ are to avoid careless squaring; absolute values bars inside the square roots suffice. Then, collecting our results,

$$\psi_{\beta su} = e^{-iEt + ip_3 z} \begin{pmatrix} u G_- \begin{pmatrix} C_{-+} \phi_{n-\bar{\beta}} \\ s^- C_{--} \phi_{n-\bar{\beta}} \end{pmatrix} \\ G_+ \begin{pmatrix} C_{++} \phi_{n-\bar{\beta}} \\ s^+ C_{+-} \phi_{n-\bar{\beta}} \end{pmatrix} \end{pmatrix}, \quad (36)$$

$$s^\sigma = -\text{sgn} \left(\frac{E^2 - \Lambda^2 + 2\tau X}{b_0 - \sigma\tau b_3} \right) = \sigma \text{sgn} \left(\frac{(\tilde{p} - \sigma b)^2 - m^2}{E(E^2 - \Lambda^2) - 2b_3 X} \right), \quad (37)$$

$$u = \sigma \text{sgn} \left(\frac{(\tilde{p} + \sigma b)^2 - m^2}{b_0 + \sigma b_3} \right) = \text{sgn} \left(\frac{E^2 - \Lambda^2 + 2X}{E(E^2 - \Lambda^2) - 2b_3 X} \right), \quad (38)$$

$$(E^2 - \Lambda^2)^2 = 4(X^2 + b^2 2n|qB|). \quad (39)$$

We call u and $s = s^+$ the $u-$ and $s-$ helicity of ψ .

For the $n = 0$ case, define

$$G_{\beta\sigma} = \sqrt{\frac{E - \beta b_3 + \sigma\beta(p_3 - \beta b_0)}{2(E - \beta b_3)}} \quad (40)$$

so that

$$\psi_\beta^{(0)} = e^{-iEt + ip_3 z} \begin{pmatrix} \text{sgn}(E - \beta b_3) G_{\beta-} \\ G_{\beta+} \end{pmatrix} \otimes \begin{pmatrix} \frac{1+\beta}{2} \phi_{n-\bar{\beta}} \\ \frac{1-\beta}{2} \phi_{n-\bar{\beta}} \end{pmatrix}. \quad (41)$$

When $n = 0$, the dispersion relation is

$$E^2 - \Lambda^2 - 2\beta X = 0, \quad (42)$$

which reduces $C_{\sigma\tau} \rightarrow \delta_{\tau\beta}$ and $G_\sigma \rightarrow G_{\beta\sigma}$ (after using absolute values to get rid of the s^σ 's).

We have defined the signs s^σ and u by assuming that the solution to the dispersion (17) is known. We have called these the u - and s -helicity above, for good reason. A straightforward computation yields

$$\begin{aligned} \frac{1}{m} \int d^3x \bar{\psi} \Sigma^3 \psi &= \frac{2X}{E(E^2 - \Lambda^2) - 2b_3 X} \\ &\stackrel{b_3=0}{=} \frac{s p_3}{E \sqrt{p_3^2 + 2n|qB|}} \\ &\stackrel{b_0=0}{=} \frac{u}{\sqrt{E^2 - 2n|qB|}}, \end{aligned} \quad (43)$$

showing that in these cases s and u become helicity and spin. In [44], the authors identified

$$\mathcal{S} = -2\gamma^5(b \cdot i\partial - m\beta) \quad (44)$$

as an operator whose eigenvalues distinguish eigenspinors in the case $b_0 = 0$. Our spinors are indeed eigenspinors of \mathcal{S} , with eigenvalue $2\xi\sqrt{(b \cdot \tilde{p})^2 - m^2 b^2}$, where $\xi = \text{sgn}(p^2 + b^2 - m^2)$. In special cases, we find

$$\begin{aligned} \xi &\stackrel{b_3=0}{=} \text{sgn}\left(b_0^2 - p_3 b_0 \sqrt{p_3^2 + 2n|qB|}\right) \\ &\stackrel{b_0=0}{=} \text{sgn}(ub_3). \end{aligned} \quad (45)$$

However, we have been unable to find a pair of operators which directly gives u and s (or some product thereof) in the general setting.

C. Limiting Cases

Here we gather the results of setting b_0 or b_3 to 0. It should be noted that these operations do not commute, for the reasons discussed above. We also include the case $m = 0$.

1. $b_3 = 0$

In this case the dispersion is

$$E = u\sqrt{m^2 + (|\mathbf{p}| - sb_0)^2}, \quad (46)$$

where $|\mathbf{p}| = \sqrt{p_3^2 + 2n|qB|}$ (and $n = 0$ only allowing $s = \beta$), and the spinor coefficients are

$$\begin{aligned} G_\sigma &= \frac{1}{2} \sqrt{\frac{E - \sigma b_0 + \sigma s |\mathbf{p}|}{E |\mathbf{p}|}}, & C_{\sigma\tau} = C_\tau &= \sqrt{|\mathbf{p}| + \tau s p_3}, \\ s^\sigma &= s = -\text{sgn}(b_0(E^2 - \Lambda^2)), & u &= \text{sgn}(E). \end{aligned} \quad (47)$$

These were also derived by [43]. Apart from s , this is well-defined in the subsequent limit $b_0 \rightarrow 0$, where s can be replaced with helicity.

$$2. \quad b_0 = 0$$

In this case the dispersion is

$$E = \pm \sqrt{2n|qB| + \left(\sqrt{m^2 + p_3^2} + ub_3 \right)^2}, \quad (48)$$

(with $n = 0$ only allowing $u = \beta$) and the spinor coefficients are

$$G_\sigma = \frac{1}{2} \sqrt{\frac{\sqrt{m^2 + p_3^2} + \sigma up_3}{|E| \sqrt{m^2 + p_3^2}}}, \quad C_{\sigma\tau} = C_\tau = \sqrt{|E| + \tau \operatorname{sgn}(E) \left(b_3 + u \sqrt{m^2 + p_3^2} \right)}, \quad (49)$$

$$G^\sigma = \sigma \operatorname{sgn}(E), \quad u = \operatorname{sgn}(b_3) \operatorname{sgn}(E^2 - \Lambda^2 - 2b_3^2).$$

These are also well-defined when $b_3 \rightarrow 0$, provided u is replaced with spin. Notice that the limits $b_0 \rightarrow 0$ and $b_3 \rightarrow 0$ do not commute; they recover solutions to the ordinary Dirac equation that are eigenspinors of different operators.

$$3. \quad m = 0$$

In this case the Dirac equation fully decouples the left- and right-chiral parts of the Dirac spinor, leaving $\Pi_\sigma \chi_\sigma = 0$. This simplifies the analysis considerably. The resulting dispersion relation is

$$E = -\sigma b_0 + r \sqrt{(\sigma p_3 + b_3)^2 + 2n|qB|}, \quad (50)$$

with $r = \operatorname{sgn}(E + \sigma b_0)$. In the special case $n = 0$, only $r = \beta$ is allowed. The corresponding eigenspinors (for any n) are

$$\psi_{r\sigma} = e^{-iEt + ip_3 z} \begin{pmatrix} \frac{1-\sigma}{2} \chi_- \\ \frac{1+\sigma}{2} \chi_+ \end{pmatrix}, \quad \chi_\sigma = \begin{pmatrix} M_{\sigma+} \phi_{n+\frac{1-\beta}{2}} \\ r\sigma M_{\sigma-} \phi_{n+\frac{1+\beta}{2}} \end{pmatrix}$$

$$M_{\sigma\tau} = \sqrt{\frac{E + \sigma b_0 + \tau(\sigma p_3 + b_3)}{2(E + \sigma b_0)}}. \quad (51)$$

It should be noted that in these expressions, the only effect of b_μ is to shift p_μ by σb_μ .

D. Choosing a Gauge

We now choose $a = 1/2$, i.e. the symmetric gauge $A_\mu = \frac{1}{2}B(0, y, -x, 0)$. This gauge is best treated with cylindrical coordinates (r, ϕ, z) , though the coordinate $\rho = \frac{|qB|}{2}r^2$ is more useful than

r . The eigenfunctions ϕ_n in this gauge are

$$\phi_n = \begin{pmatrix} \phi_n^{(1)} \\ \phi_n^{(2)} \end{pmatrix} \sim e^{ij\phi} \begin{pmatrix} e^{-i\phi/2} I_{n-\frac{1-\beta}{2}, a} \\ -i\beta e^{i\phi/2} I_{n-\frac{1+\beta}{2}, a} \end{pmatrix}, \quad (52)$$

with $j = \beta(a - n + 1/2)$ the z -angular momentum quantum number and a now a nonnegative integer. The functions $I_{n,a}(\rho)$ are the Laguerre functions

$$I_{n,a}(\rho) = \sqrt{\frac{a!}{n!}} e^{-\rho/2} \rho^{\frac{n-a}{2}} L_a^{(n-a)}(\rho), \quad (53)$$

with $L_a^{(n-a)}(\rho)$ an associated Laguerre polynomial. In the previous section we ignored the two-component nature of ϕ_n as well as the index j . Rest assured, these take care of themselves: see Appendix B. The two-component spinors of the previous section are then

$$\chi_{\sigma}^{(n)} = e^{ij\phi} \begin{pmatrix} C_{\sigma+} e^{-i\phi/2} I_{n-\frac{1-\beta}{2}, a} \\ -i\beta s^{\sigma} C_{\sigma-} e^{i\phi/2} I_{n-\frac{1+\beta}{2}, a} \end{pmatrix}. \quad (54)$$

The functional form is identical to the $b_{\mu} = 0$ case; the only difference is in the coefficients $C_{\sigma\tau}$ and G_{σ} . The same would be true if we had chosen the Landau gauge $a = 1$.

E. Chiral magnetic current

In Appendix A, we use the solutions to the Dirac equation with finite b_0 and b_3 (56) that we derived in this section to compute the chiral magnetic current. We verify that the computed current does not depend on b_3 , as expected.

III. SYNCHROTRON RADIATION

We now move to computing the synchrotron radiation emitted from the fermions described above. The \mathcal{S} -matrix element we wish to compute is

$$\mathcal{S} = \int \psi_{s'u'\beta}^{(n')\dagger} i q \mathcal{A}^* \psi_{su\beta}^{(n)} d^4x. \quad (55)$$

The Dirac spinors, properly normalized, are

$$\psi_{su\beta} = e^{-irEt+ip_3z+ij\phi} \sqrt{\frac{|qB|}{2\pi L}} \begin{pmatrix} C_1 e^{-i\phi/2} I_1 \\ -i\beta C_2 e^{i\phi/2} I_2 \\ C_3 e^{-i\phi/2} I_1 \\ -i\beta C_4 e^{i\phi/2} I_2 \end{pmatrix} = e^{-irEt+ip_3z+ij\phi} \sqrt{\frac{|qB|}{2\pi L}} \chi, \quad (56)$$

We have written

$$I_1(\rho) = I_{n-\frac{1-\beta}{2},a}(\rho), \quad I_2(\rho) = I_{n-\frac{1+\beta}{2},a}(\rho), \quad (57)$$

and C_i for the coefficients determined in the previous section (not to be confused with $C_{\sigma\tau}$).

The photon wavefunctions, with helicity h , z -angular momentum ℓ , and momentum \mathbf{k} , are

$$\begin{aligned} \mathbf{A}_{h,\ell,\mathbf{k}}(x) &= \frac{1}{\sqrt{2\omega V}} \Phi_{h,\ell,\mathbf{k}}(\mathbf{x}) e^{-i\omega t}, & \Phi_{h,\ell,\mathbf{k}}(\mathbf{x}) &= \frac{1}{2} (h\mathbf{T} + \mathbf{P}) e^{ik_z z + i\ell\phi}, \\ \mathbf{T} &= \frac{i\ell}{k_{\perp} r} J_{\ell}(k_{\perp} r) \hat{r} - J'_{\ell}(k_{\perp} r) \hat{\phi}, & \mathbf{P} &= \frac{ik_z}{k} J'_{\ell}(k_{\perp} r) \hat{r} - \frac{\ell k_z}{kk_{\perp} r} J_{\ell}(k_{\perp} r) \hat{\phi} + \frac{k_{\perp}}{k} J_{\ell}(k_{\perp} r) \hat{z}. \end{aligned} \quad (58)$$

The calculation is the same as in the $b_0 = b_3 = 0$ case (a classic reference is [54]; we recently reviewed the calculation, with modern notation, in [34]). A straightforward but tedious calculation, whose only non-trivial step is an integral identity [55], brings us to

$$\mathcal{S} = 2\pi\delta(E - E' - \omega) \frac{2\pi}{L} \delta(p_3 - p'_3 - k_z) \delta_{l,j-j'} \beta^{m-m'} I_{a,a'}(x) \frac{-iq}{\sqrt{2\omega V}} \langle \mathbf{j} \cdot \Phi \rangle, \quad (59)$$

with

$$\sqrt{2} \langle \mathbf{j} \cdot \Phi \rangle = -K_1(h - \cos\theta) I_{n-1,n'} + K_2(h + \cos\theta) I_{n,n'-1} + \sin(\theta) (K_3 I_{n,n'} - K_4 I_{n-1,n'-1}) \quad (60)$$

for $\beta = +1$; for $\beta = -1$, switch $n \leftrightarrow n - 1$ and $n' \leftrightarrow n' - 1$. The coefficients K_i are

$$\begin{aligned} K_1 &= C'_3 C_4 - C'_1 C_2, & K_2 &= C'_4 C_3 - C'_2 C_1, \\ K_3 &= C'_3 C_3 - C'_1 C_1, & K_4 &= C'_4 C_4 - C'_2 C_2. \end{aligned} \quad (61)$$

From here, we compute the differential rate

$$\frac{d\dot{w}}{d\Gamma d\Gamma' d\Gamma_k} = \frac{|\mathcal{S}|^2}{T} = \frac{q^2}{2\omega V} 2\pi\delta(E - E' - \omega) \frac{2\pi}{L} \delta(p_3 - p'_3 - k_z) \delta_{l,j-j'} I_{a,a'}^2 |\langle \mathbf{j} \cdot \Phi \rangle|^2, \quad (62)$$

with T a formal symbol to cancel a factor of $2\pi\delta(E - E' - \omega)$ (also called the observation time). $d\Gamma = \frac{d^3 x d^3 k}{(2\pi)^3}$ is a phase space differential for the initial fermion and $d\Gamma'$ and $d\Gamma_k$ are the same for the final fermion and photon. Integrating the photon volume and final fermion phase spaces, we find

$$\frac{d\dot{w}}{d\Gamma d^3 k} = \frac{q^2}{4\pi} \frac{1}{2\pi\omega} \sum_{n',a'} \delta_{l,j-j'} I_{a,a'}(x)^2 |\langle \mathbf{j} \cdot \Phi \rangle|^2 \delta(E - E' - \omega), \quad (63)$$

with $p'_3 = p_3 - k_z$, and we have used the substitution

$$d\Gamma' \rightarrow \frac{1}{A} \sum_{n',a'} \int \frac{dp'_3}{2\pi} \quad (64)$$

appropriate to the Landau level description [56]. A is the area of the extent of our spatial cylinder, canceled by the integration $\int d^3x' = V$. The same will be done for $d\Gamma$ later. We will use another trick for the photon momentum:

$$\int d^3k \delta_{l,j-j'} = 2\pi \sum_l \delta_{l,m-m'} \int dk_z dk_{\perp} k_{\perp} = 2\pi \int dk_z dk_{\perp} k_{\perp} = \int d^3k, \quad (65)$$

where we have used the azimuthal symmetry of the problem in the last equality. Then we can use the identity [54]

$$\sum_{a'} I_{a,a'}^2(x) = 1 \quad (66)$$

to find the differential photon emission rate:

$$\frac{d\dot{w}}{d\Gamma d^3k} = \frac{q^2}{4\pi} \frac{1}{2\pi\omega} \sum_{n'} |\langle \mathbf{j} \cdot \Phi \rangle|^2 \delta(E - E' - \omega), \quad (67)$$

evaluated with $p'_3 = p_3 - k_z$. We have suppressed the potential dependence on the final state's helicity quantum numbers, which are not specified by fixing p'_3 and n' . The photon helicity dependence is also suppressed, but this dependence is easily computable given the expression for the matrix elements.

A. Single-particle radiation

Here we evaluate the radiation intensity W , the radiated energy per unit time, from a single particle, i.e.

$$W(E, n, p_3) = \int d^3k \omega \frac{d\dot{w}}{d\Gamma d^3k} \quad (68)$$

for a specified initial state with quantum numbers E, n, p_3 . Writing out the rate integral,

$$\dot{w}(E, n, p_3) = \frac{q^2}{4\pi} \sum_{n'} \int d\omega d\cos\theta \omega |\langle \mathbf{j} \cdot \Phi \rangle|^2 \delta(E - E' - \omega) \quad (69)$$

(we have dropped $d\Gamma$ in favor of the functional dependence (E, n, p_3)). The Dirac delta can be converted to fix ω with the factor

$$\delta(E - E' - \omega) = \frac{\delta(\omega - \omega_0)}{\left|1 + \frac{\partial E'}{\partial \omega}\right|} = \delta(\omega - \omega_0) |\Delta|, \quad (70)$$

$$\Delta = \frac{E'(E'^2 - \Lambda'^2) - 2b_3 X'}{(E' - p'_3 \cos\theta)(E'^2 - \Lambda'^2) - 2(b_3 - b_0 \cos\theta)X'}, \quad (71)$$

where ω_0 is the solution to $E = E' + \omega$. Multiple solutions may exist, corresponding to different values of $s^{\sigma'}$ and u' . The result is

$$W(E, n, p_3) = \frac{q^2}{4\pi} \sum_{n'} \int d\cos\theta \omega_0^2 |\langle \mathbf{j} \cdot \Phi \rangle|^2 |\Delta|. \quad (72)$$

We compute this quantity numerically in Section IV A.

B. Plasma radiation

To compute the radiation from a non-interacting plasma, we go back to Eq. (62) and apply Fermi-Dirac statistical weight factors. Since the manipulations leading to Eq. (67) are not affected by this, we can proceed from there. We again use the Landau level prescription for the transverse momentum integration. The Dirac delta can be converted to integrate p_3 immediately,

$$\delta(E - E' - \omega) = \frac{\delta(p_3 - p_3^0)}{\left| \frac{\partial E}{\partial p_3} - \frac{\partial E'}{\partial p_3'} \right|} = \delta(p_3 - p_3^0) |\Delta|, \quad (73)$$

$$\Delta = \frac{(E(E^2 - \Lambda^2) - 2b_3 X)(E'(E'^2 - \Lambda'^2) - 2b_3 X')}{(p_3 E' - p_3' E)(E^2 - \Lambda^2)(E'^2 - \Lambda'^2) + 2(\tilde{p} \cdot b X'(E^2 - \Lambda^2) - \tilde{p}' \cdot b X(E'^2 - \Lambda'^2))}, \quad (74)$$

where p_3^0 is a solution to the energy-momentum conservation. Then the number of photons emitted from the plasma per unit time per unit volume for given \mathbf{k} is

$$\frac{dN}{dtdVd^2k_{\perp}dy} = \frac{q^2}{4\pi} \frac{1}{(2\pi)^2} \frac{|qB|}{2\pi} \sum_{n, n', p_3^0} |\Delta| f(E) f(-E') |\langle \mathbf{j} \cdot \Phi \rangle|^2. \quad (75)$$

We have changed coordinates to those used in heavy-ion collisions and multiplied by ω in anticipation of the next section. We are only interested in $y = 0$, i.e. the plane perpendicular to the collision axis, where $k_T = \omega$ and $\phi = \pi - \theta$. The sum over p_3^0 is a sum over solutions to the energy-momentum conservation condition. The integrated quantities we wish to compute are

$$v_0 = \left\langle \frac{dN}{d^2k_{\perp}dy} \Big|_{y=0} \right\rangle = \frac{q^2}{4\pi} \frac{L\Delta t}{(2\pi)^2} \frac{1}{2\pi} \int_0^{2\pi} d\phi \frac{dN}{d^2k_{\perp}dy} \Big|_{y=0}, \quad (76)$$

$$v_2 = \frac{1}{v_0} \frac{1}{2\pi} \int_0^{2\pi} d\phi \cos(2\phi) \frac{dN}{d^2k_{\perp}dy} \Big|_{y=0}. \quad (77)$$

Using the rotational symmetry about the \mathbf{B} axis, the ϕ integration can be carried out over $(-\pi/2, \pi/2)$, then multiplied by 2. L and Δt are the length of the cylinder of plasma and the observation time interval, roughly the longitudinal size and lifetime of the plasma. We compute these quantities numerically in Section IV B

IV. SYNCHROTRON RADIATION BY QGP AT FINITE b_0 AND b_3

In this section, we present results from the numerical calculations of synchrotron radiation from a single particle (Eq. (72)) and for v_0 and v_2 of a non-interacting plasma of fermions (Eqs. (76) and (77)) in the presence of nonzero chiral chemical potential b_0 and chiral gradient b_3 . The single-particle radiation is somewhat academic, but hints at the results for v_0 . The plasma radiation is presented alongside data from the PHENIX detector at RHIC [57–60].

We use a fermion mass of $m = 300$ MeV. This corresponds to the thermal mass of quarks in the QGP, where the thermal mass is $m^2 = \frac{g^2 T^2}{16 N_c} (N_c^2 - 1)$.

The chiral chemical potential in relativistic heavy-ion collisions can be as large as 100 MeV [61–64]. We assume that the chiral gradient b_3 may have similar order of magnitude. The numerical calculations presented in this section explore a range of parameters.

A. Single-particle radiation

The calculation of Eq. (72) numerically is straightforward. We choose an initial value of n and p_3 , specifying the momentum of the (single) initial particle, then solve the dispersion relation, Eq. (17), numerically.³ For each n' , we numerically solve the energy-momentum conservation condition for the photon energy ω , then compute the matrix element. The sum on n' is finite due to kinematic constraints. b_0 and b_3 do allow for additional transitions, but their effect is small. We normalize the intensity W to the classical result

$$W_{\text{Cl}}(E) = \frac{2}{3} \frac{(qB)^2 E^2}{m^4}. \quad (78)$$

It should be noted that the value of B used here, as in our previous work [33, 34], is not small enough that we expect our results to approach the ratio 1.

Figs. 1 and 2 show the single-particle radiation intensity as a function of the initial particle energy E for fixed values of $p_3 = 0$, $m = 300$ MeV, and $qB = 0.01m^2 = 900$ MeV². This value is sufficiently large to facilitate computations for high energies ($E \approx 15m = 4500$ MeV) while still being in a regime well-described by semiclassical calculations. We found that changing p_3 does not affect any qualitative features of the spectrum.

We note especially the splitting of the radiation from initial particles of opposite $s-$ or $u-$ helicity. Recall that these are the parameters which distinguish the energy eigenvalues, and

³ The quartic dispersion of course has a solution in terms of radicals, but it is cumbersome to write out, and solving the energy conservation condition for ω is slower when using these formulae than doing so numerically.

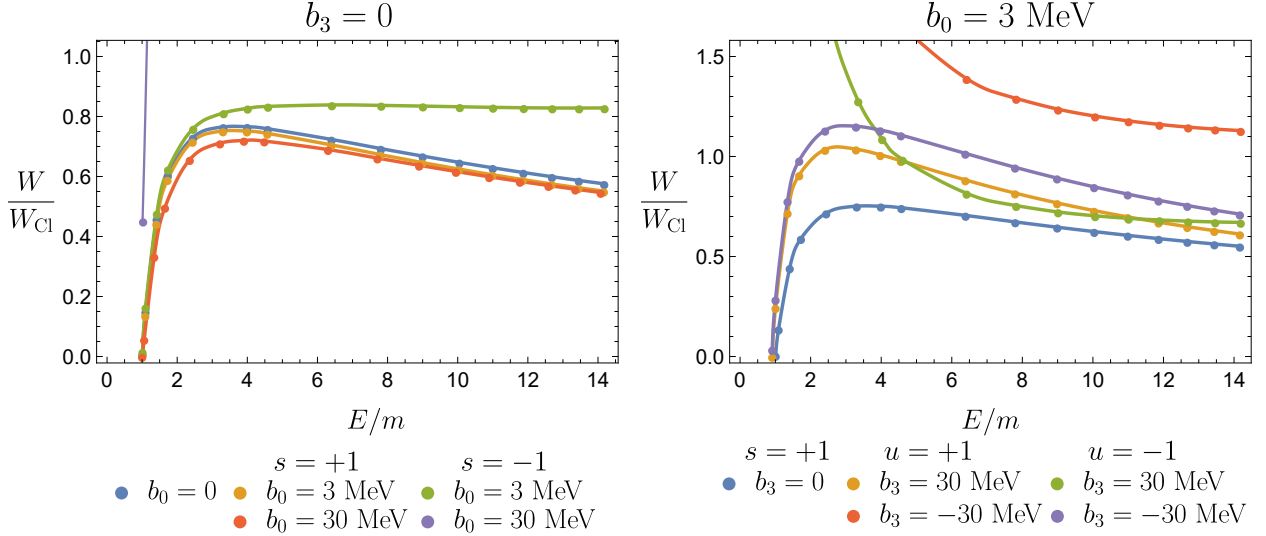


FIG. 1. The single-particle radiation intensity due to a magnetic field $qB = 0.01m^2 = 900 \text{ MeV}^2$. Left: The chiral chemical potential $\mu_5 = b_0$ is varied while $b_3 = 0$ is fixed. Right: $\mu_5 = b_0 = 3 \text{ MeV}$ is fixed while b_3 varies. The blue curve in the left figure is the $b_0 = b_3 = 0$ result, well-approximated by standard semiclassical computations [34]. Differences in s - and u -helicity have been made apparent.

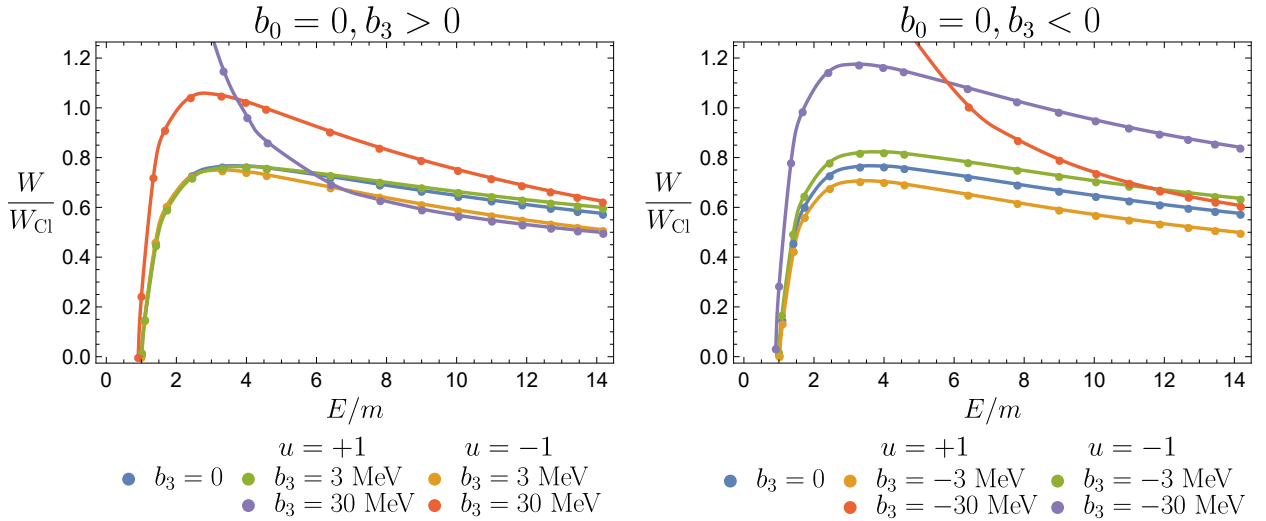


FIG. 2. The same as Figure 1, but for various values of b_3 with $\mu_5 = b_0 = 3 \text{ MeV}$. The difference due to the sign of b_3 is evident.

reduce to ordinary helicity and the sign of E when either b_0 or b_3 is set to 0. The splitting is due to the fact that, even when $b_0 = b_3 = 0$, there is a small difference in radiation when the initial spin is parallel or antiparallel to $q\mathbf{B}$. Since s and u correspond to spin eigenvalues in this case, this feature is unsurprising. b_0 and b_3 increase this difference due to the broken degeneracy. When these parameters are larger, the effect is greater. We have neglected to show the full extent of

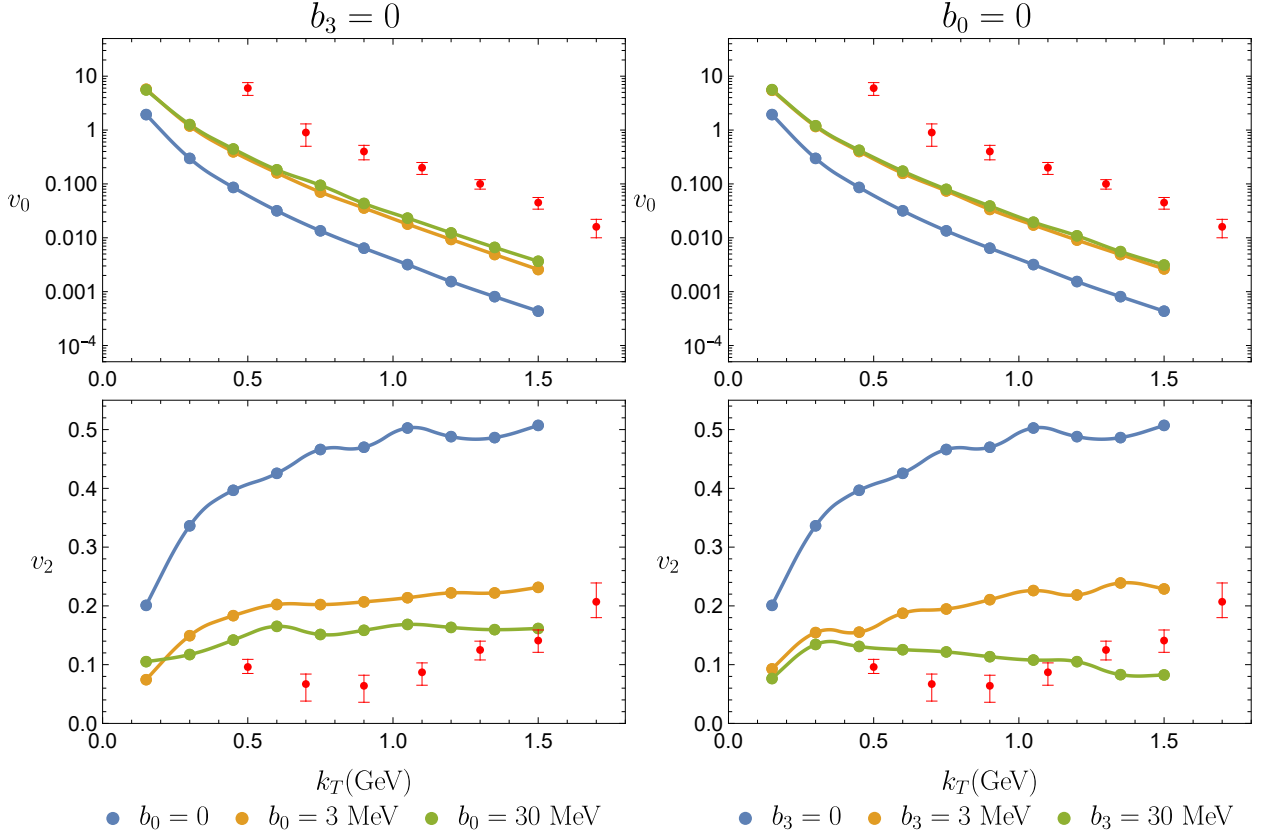


FIG. 3. v_0 and v_2 for the photon spectrum of a plasma of up and down quarks with temperature $T = m = 300$ MeV. $b_0 = \mu_5$ is a chiral chemical potential. The magnetic field is $|e|B = m_\pi^2 = 18000$ MeV 2 . We have estimated $L = c\Delta t = 10$ fm. The red points are 20-40% centrality results from the PHENIX collaboration [57–60].

the resulting radiation in the low-energy regime. This enhancement is due to entering a different kinematic regime which is normally accessible by increasing the magnetic field.

The right panel of Fig. 1 shows the interplay of the two parameters. Having fixed $b_0 = 3$ MeV, we can see the further effect of including b_3 in the calculation. However, there is little not present in the previous discussion.

B. Plasma radiation

The calculation of v_0 and v_2 numerically is done in two steps. We first compute the differential rate given by Eq. (75) for fixed ω as a function of θ , the spherical polar coordinate, then integrate to get either quantity. To compute a summand, for given n, n', ω , and θ we solve the dispersions for the initial and final particle numerically for E and p_3 by imposing energy-momentum conservation

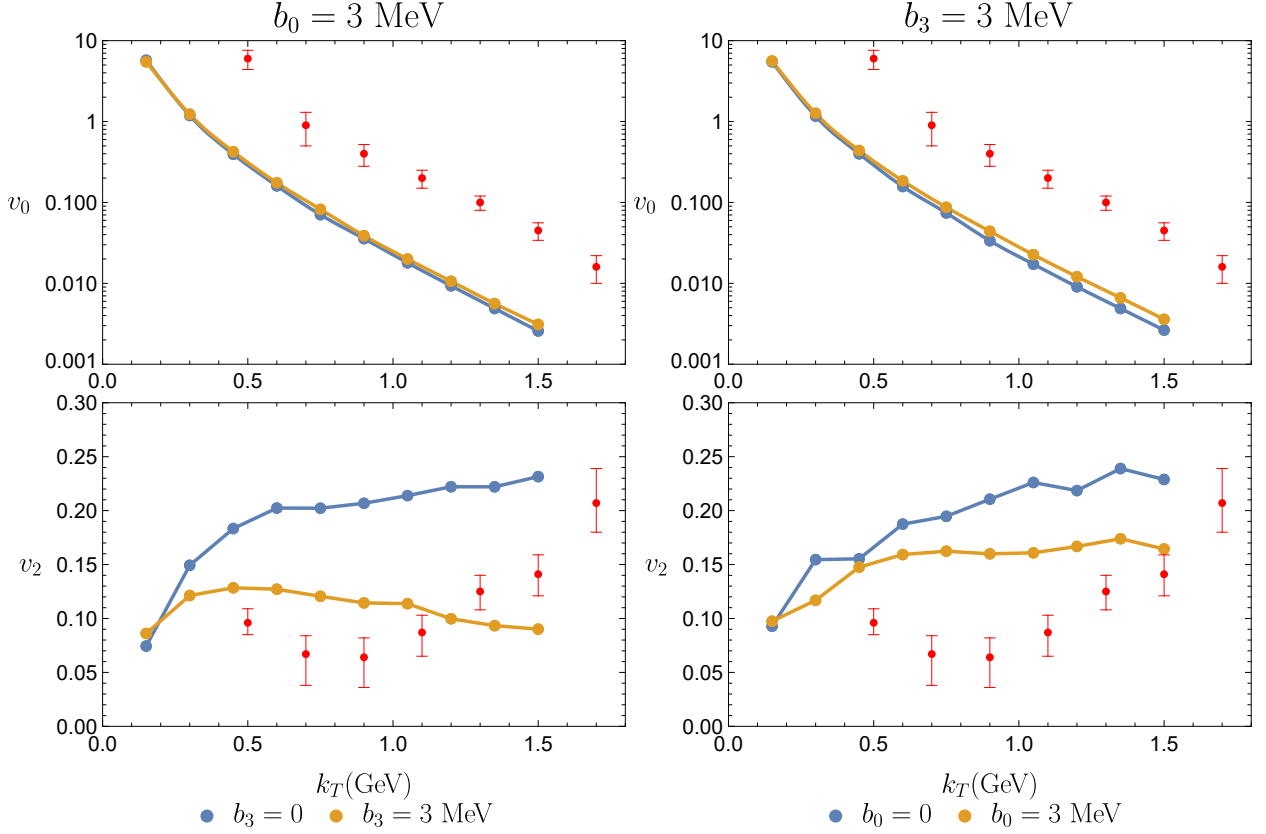


FIG. 4. The same as Fig. 3, but with both $b_0 = \mu_5$ and b_3 turned on. Left: $b_0 = 3$ MeV is fixed. Right: $b_3 = 3$ MeV is fixed. We have estimated $L = c\Delta t = 10$ fm. The red points are 20-40% centrality results from the PHENIX collaboration [57–60].

on the dispersion for E' .⁴ Then the summand can be computed.

Since the limits of the sum over n is in principle infinite, we have to cut it off. We do this by summing over 100 initial-state Landau levels at a time, then checking to see if the sum has converged. We stop when the next 100 levels gives less than a 1% difference in v_0 . In practice, this required no more than the first 1000 initial-state Landau levels for the magnetic field strengths used. The sum over n' for given n terminates, as in the single-particle case. We again include the additional transitions allowed by b_0 and b_3 , but their effect is small, and they do not contribute any qualitative features to the spectrum of the thermal plasma.

Figure 3 shows v_0 and v_2 for a plasma of up and down quarks and antiquarks in a magnetic field of $|e|B = m_\pi^2 = 18000$ MeV². We have used $m = T = 300$ MeV as our mass scale. In computing v_0 , we had to choose a length and time scale to compare with experimental data; we chose $L = c\Delta t = 10$ fm, about the length and lifetime of the QGP. The effect of either parameter on

⁴ Even when b_0 or b_3 are 0, and hence E can be written succinctly, it is not trivial to write down p_3^0 , so we still do this step numerically in these cases.

v_0 is an increase in the number of photons produced by a factor of about 4, depending on p_T . The effect seems to saturate when either parameter is on the order $10^{-2}m = 3$ MeV. Furthermore, as Figure 4 shows, including both parameters gives little appreciable difference in photons produced when compared to including just one. The striking result is in v_2 , where a significant decrease is observed when either parameter is turned on. Turning on both parameters only seems to allow one parameter to dominate, although this may be due to the range of parameters we have explored. The result for v_2 is quite promising. First, it does not depend on the length and time scale multiplying v_0 . Also, traditional hydrodynamics simulations tend to compute v_2 to be smaller than what is observed in experiments [7, 65, 66]. Could the two results meet in the middle?

V. CONCLUSION

We have solved the modified Dirac equation (2) in the presence of a constant magnetic field, a chiral chemical potential b_0 , and a chirality gradient b_3 in the direction of the magnetic field. The solution is presented in Eq. (36). The novel result is the use of b_3 . We applied this solution to QGP phenomenology by computing synchrotron radiation from fermions in a medium with these properties and found that while the total number of photons produced (v_0) is only modestly enhanced, the traditionally large synchrotron v_2 is significantly reduced to a level comparable to experimental data.

We have demonstrated in our recent publications that plasma rotation increases the number of photons produced [31–34]. Therefore, it is reasonable to expect that the synchrotron radiation from a rotating plasma in the presence of a chiral imbalance could solve the direct photon puzzle. Such a calculation is not prohibitive: taking rotation into account only requires adding $\boldsymbol{\Omega} \cdot \mathbf{J}$ to the Hamiltonian. If the rotation axis is chosen to coincide with \mathbf{B} (which is on average true in the QGP), this operator commutes with the Hamiltonian associated with the Dirac equation we solved in this paper. The only difference, then, is the dependence of E on the angular momentum quantum number j , which only affects the kinematics [34]. It should be noted that this introduces certain numerical difficulties and the possibility of requiring new boundary conditions, but such problems have been dealt with before, both exactly [30] and with semiclassical methods [32]. Future phenomenological applications may also consider any possible changes in the photon spectrum due to plasma expansion [67, 68].

Wang and Shovkovy [53] recently published a similar calculation of synchrotron radiation emitted from a plasma of massless fermions with a chiral chemical potential. They were primarily

interested in the differences in the spectra of different photon polarizations and did not compute v_0 or v_2 . We have not directly compared to their results because in the massless limit, we find that the matrix elements for the case with $b_0 = \mu_5$ (and b_3) are identical to those for the case without them. Because the Dirac equation decouples, the only effect on the wavefunctions is to shift p_μ by b_μ . Since photon emission from massless fermions cannot induce a chirality change, the kinematics of the reaction is not affected by this shift. As a result, we find that the only difference in the photon spectrum comes from the Fermi-Dirac distribution factors in Eq. (75). In this context, our inclusion of a fermion mass (which in the QGP is a large thermal mass ~ 300 MeV) makes our work a novel result.

We investigated the role of the chiral transport coefficients b_0 and b_3 on photon production. It would be interesting to extend this study to include the transverse parameters b_1 and b_2 . This entails solving the Dirac equation for an arbitrary b_μ , a noble goal that requires a dedicated study.

ACKNOWLEDGMENTS

We thank Matteo Buzzegoli and Nandagopal Vijayakumar for many fruitful discussions and collaboration on related projects. This work was supported in part by the U.S. Department of Energy under Grant No. DE-SC0023692.

Appendix A: Chiral Magnetic Effect

Our results allow us to investigate the effect of b_3 on the chiral magnetic effect (CME). The CME current can be obtained by computing the velocity expectation value of the wavefunctions in Eq. (36). A derivation in the same spirit was present in the original paper of Fukushima et al. [69] using formal properties of the wavefunctions. Our analysis reduces this argument to a straightforward matrix multiplication.

The velocity expectation value is

$$\mathbf{v} = \int \bar{\psi}_{rs} \gamma \psi_{rs}. \quad (\text{A1})$$

Inserting the wavefunction in Eq. (56) and introducing the notation

$$\tilde{\chi}_\sigma = \begin{pmatrix} C_{\sigma+} I_1 \\ C_{\sigma-} I_2 \end{pmatrix}, \quad (\text{A2})$$

one finds

$$\mathbf{v} = \frac{|qB|}{2\pi} \int d^2x_\perp \sum_{\sigma=\pm 1} \sigma G_\sigma^2 \tilde{\chi}_\sigma^\dagger (\sigma^1 \hat{r} + \sigma^2 \hat{\phi} + \sigma^3 \hat{z}) \tilde{\chi}_\sigma. \quad (\text{A3})$$

The orthonormality of the functions $I_{p,q}(x)$ makes the \hat{r} and $\hat{\phi}$ components vanish and the \hat{z} -component integration trivial, leaving

$$\mathbf{v} = v \hat{z} = \sum_{\sigma, \tau = \pm 1} \sigma \tau G_\sigma^2 C_{\sigma\tau}^2 \hat{z}. \quad (\text{A4})$$

Evaluating the sum, one finds

$$v = \frac{p_3(E^2 - \Lambda^2) - 2b_0 X}{E(E^2 - \Lambda^2) - 2b_3 X} = \frac{\partial E}{\partial p_3}, \quad (\text{A5})$$

using the notation of Eq. (11).

The result $v = \frac{\partial E}{\partial p_3}$ is hardly surprising, and shows that the derivation of v (although not necessarily \mathbf{v}) requires only the dispersion relation, namely Eq. (17). Then one may take a thermal average,

$$\langle v \rangle = \sum_{n,a} \sum_{E_i} \int \frac{dp_3}{2\pi} \frac{\partial E_i}{\partial p_3} n_F(E_i), \quad (\text{A6})$$

with E_i the solutions to the dispersion relation for given n . We allow negative energies, as when b_0 and b_3 are non-zero, three solutions to the dispersion relation can be positive (or negative). The sum over a gives the Landau level degeneracy factor $\frac{|qB|}{2\pi}$, and the integration of p_3 gives

$$\langle v \rangle = \frac{|qB|}{2\pi} \sum_n \sum_{E_i} -T \lim_{\Lambda \rightarrow \infty} \log \left(\frac{1 + \exp(-E_i(\Lambda)/T)}{1 + \exp(-E_i(-\Lambda)/T)} \right). \quad (\text{A7})$$

The CME current J is this quantity times the charge q .

The ordinary setting for the CME has $b_3 = 0$. In this case, the energies E_i are

$$E_{rs} = r \sqrt{m^2 + \left(\sqrt{2n|qB| + p_3^2} - sb_0 \right)^2} \quad (\text{A8})$$

for $n > 0$. Evidently, $E_{rs}(\Lambda) = E_{rs}(-\Lambda)$, so all limits for $n > 0$ vanish. When $n = 0$,

$$E_r = r \sqrt{m^2 + (p_3^2 - \beta b_0)^2}, \quad (\text{A9})$$

which does not have the previous symmetry. Instead,

$$\sum_r \lim_{\Lambda \rightarrow \infty} \log \left(\frac{1 + \exp(-E_r(\Lambda)/T)}{1 + \exp(-E_r(-\Lambda)/T)} \right) = \frac{1}{T} \lim_{\Lambda \rightarrow \infty} E_+(\Lambda) - E_+(-\Lambda) = -\frac{2\beta b_0}{T}, \quad (\text{A10})$$

which gives the familiar expression

$$J = \frac{q^2 B}{2\pi^2} b_0 \quad (\text{A11})$$

for the CME current.

We now investigate whether b_3 affects the CME current. We will build up to the massive case slowly. In the setting $b_0 = 0$ and $m \neq 0$, the dispersion

$$E_{ru} = r \sqrt{2n|qB| + \left(\sqrt{m^2 + p_3^2} + ub_3 \right)^2} \quad (\text{A12})$$

has a $p_3 \rightarrow -p_3$ symmetry even when $n = 0$, so the CME current vanishes. If we allow $b_0 \neq 0$ again, but set $m = 0$, the dispersion

$$E_{r\sigma} = -\sigma b_0 + r \sqrt{(\sigma p_3 + b_3)^2 + 2n|qB|} \quad (\text{A13})$$

has the symmetry $E_{\sigma r}(p_3) = -E_{-\sigma-r}(-p_3)$ for $n > 0$, so all of these terms vanish in the sum. For $n = 0$,

$$E_\sigma = -\sigma b_0 + \beta(\sigma p_3 + b_3). \quad (\text{A14})$$

The sum is more involved in this case, but one finds that all contributions from b_3 cancel, and

$$J = \frac{q^2 B}{2\pi^2} b_0 \quad (\text{A15})$$

With b_0, b_3 , and m all nonzero, the lack of a compact solution $E = \dots$ to the dispersion relation presents a difficulty. However, we are only interested in the limit $|p_3| \rightarrow \infty$, so an asymptotic form will suffice. A tedious analysis shows

$$E_{r\tau} = r \left(p_3 + \frac{m^2 + 2n|qB|}{2p_3} \right) - \tau(b_0 - rb_3) \quad (\text{A16})$$

for $n > 0$. Putting this into Eq. (A7), we find that the $n > 0$ levels contribute 0 to the CME current. The $n = 0$ case is much more straightforward, as

$$E_r = \beta b_3 + r \sqrt{(p_3 - \beta b_0)^2 + m^2}, \quad (\text{A17})$$

which goes through in almost the same way as the $b_3 = 0$ case to yield

$$J = \frac{q^2 B}{2\pi^2} b_0. \quad (\text{A18})$$

Thus b_3 does not affect the CME. This result is hardly surprising, given that it is known that \mathbf{b} induces a current $\mathbf{b} \times \mathbf{E}$, and we have no electric field in this setting. The calculation is nonetheless both instructive and reassuring.

Appendix B: Landau Level Wavefunctions

In this appendix, we show a few details concerning the spatial eigenfunctions $\phi_n(\mathbf{x}_\perp)$ used in the main text.

The first item is the fact that $D_\pm^\perp = iD_1 \mp D_2$ serve as raising and lowering operators for the functions ϕ_n in a constant magnetic field $\mathbf{B} = B\hat{z}$. This can be seen from the fact that

$$[D_+^\perp, D_-^\perp] = 2qB, \quad (\text{B1})$$

which, after relabeling

$$\hat{a}_\beta = \frac{-1}{\sqrt{2|qB|}}(iD_1 - \beta D_2) = \frac{-1}{\sqrt{2|qB|}}D_\beta^\perp, \quad \hat{a}_\beta^\dagger = \frac{-1}{\sqrt{2|qB|}}(iD_1 + \beta D_2) = \frac{-1}{\sqrt{2|qB|}}D_{-\beta}^\perp, \quad (\text{B2})$$

yields $[\hat{a}_\beta, \hat{a}_\beta^\dagger] = 1$. This signals the algebra of a simple harmonic oscillator.

To write a solution to the Dirac equation, we are forced to choose a gauge: we choose the symmetric gauge, in which cylindrical coordinates (r, ϕ, z) are most useful. In this gauge,

$$\hat{a}_\beta = ie^{i\beta\phi}\frac{\sqrt{\rho}}{2}\left(2\partial_\rho + \frac{i\beta}{\rho}\partial_\phi + 1\right), \quad \hat{a}_\beta^\dagger = ie^{-i\beta\phi}\frac{\sqrt{\rho}}{2}\left(2\partial_\rho - \frac{i\beta}{\rho}\partial_\phi - 1\right), \quad (\text{B3})$$

where $\rho = |qB|r^2/2$. Since we seek spinor solutions, things are a bit trickier. Here we only sketch the solutions, but we recently gave more detail in [34]. Since $\gamma^0\gamma^5\mathbb{b}$ (the term in the Hamiltonian corresponding to (2)) commutes with J_z , we expect

$$\psi_n(\mathbf{x}_\perp) = e^{ij\phi} \begin{pmatrix} e^{-i\phi/2}f_1(r) \\ e^{i\phi/2}f_2(r) \\ e^{-i\phi/2}f_3(r) \\ e^{i\phi/2}f_4(r) \end{pmatrix} = e^{im\phi}e^{-i\Sigma^3\phi/2}\mathbf{f}. \quad (\text{B4})$$

The resulting differential equation for the f_i shows that up to the constants derived in the main text, $f_1(r) = f_3(r)$ and $f_2(r) = f_4(r)$. These solve the differential equations

$$\hat{a}_\beta^\dagger \hat{a}_\beta f(r) = -2|qB|f(r), \quad \hat{a}_\beta \hat{a}_\beta^\dagger f(r) = -2|qB|f(r), \quad (\text{B5})$$

(which functions solve which equation depends on β), whose solutions are the Laguerre functions

$$I_{n,a}(\rho) = \sqrt{\frac{a!}{n!}}e^{-\rho/2}\rho^{(n-a)/2}L_a^{(n-a)}(\rho), \quad (\text{B6})$$

with $a = \beta j + n - 1/2$ and $L_a^{(n-a)}(\rho)$ a generalized Laguerre polynomial. The recurrence relations of the Laguerre polynomials imply that

$$D_\tau^\perp e^{i(j-\tau/2)\phi} I_{n-(1-\tau\beta)/2,a}(\rho) = i\tau\beta\sqrt{2n|qB|}e^{i(j+\tau/2)\phi} I_{n-(1+\tau\beta)/2,a}(\rho). \quad (\text{B7})$$

This is nearly the statement of Eq. (8), once we assemble our results properly. The spatial eigenspinors are

$$\phi_n^\sigma(\mathbf{x}_\perp) = e^{ij\phi} e^{-i\sigma^3\phi/2} \begin{pmatrix} c_n^\sigma I_{n-\frac{1-\beta}{2},a}(\rho) \\ -i\beta d_n^\sigma I_{n-\frac{1+\beta}{2},a}(\rho) \end{pmatrix}. \quad (\text{B8})$$

The coefficients c_n^σ and d_n^σ are those derived in the text. The full wavefunction is $\psi_n = (f_n \phi_n^- \ g_n \phi_n^+)^T$.

The second item is that we did not use the spinor nature of ϕ_n^σ to find the coefficients of the Dirac spinor. The main jump was getting from Eq. (7) to Eq. (10). For simplicity, set $\beta = -1$, and look only at the first row of Eq. (7), applied to the expansion in the eigenspinors ϕ_n^σ . Eq. (B7) shows that

$$D_-^\perp D_+^\perp \phi_n^{\sigma(1)} = 2n|qB|c_n^\sigma e^{i(j-1/2)\phi} I_{n,a}(\rho), \quad (\text{B9})$$

and that

$$D_-^\perp \phi_n^{\sigma(2)} = D_-^\perp i d_n^\sigma e^{i(j+1/2)\phi} I_{n,a} = -\sqrt{2n|qB|} d_n^\sigma e^{i(j-1/2)\phi} I_{n-1,a} = -\sqrt{2n|qB|} \frac{d_n^\sigma}{c_n^\sigma} \phi_n^{\sigma(1)}. \quad (\text{B10})$$

The second row of Eq. (7) proceeds similarly. The indices are dizzying, but this is exactly what leads to Eq. (10).

- [1] P. B. Arnold, G. D. Moore, and L. G. Yaffe, Photon emission from quark gluon plasma: Complete leading order results, *JHEP* **12**, 009, arXiv:hep-ph/0111107.
- [2] J. Ghiglieri, J. Hong, A. Kurkela, E. Lu, G. D. Moore, and D. Teaney, Next-to-leading order thermal photon production in a weakly coupled quark-gluon plasma, *JHEP* **05**, 010, arXiv:1302.5970 [hep-ph].
- [3] C. T. Traxler, H. Vija, and M. H. Thoma, Hard photon production rate of a quark - gluon plasma at finite quark chemical potential, *Phys. Lett. B* **346**, 329 (1995), arXiv:hep-ph/9410309.
- [4] J.-F. Paquet, C. Shen, G. S. Denicol, M. Luzum, B. Schenke, S. Jeon, and C. Gale, Production of photons in relativistic heavy-ion collisions, *Phys. Rev. C* **93**, 044906 (2016), arXiv:1509.06738 [hep-ph].
- [5] H. van Hees, C. Gale, and R. Rapp, Thermal Photons and Collective Flow at the Relativistic Heavy-Ion Collider, *Phys. Rev. C* **84**, 054906 (2011), arXiv:1108.2131 [hep-ph].
- [6] C. Shen, U. W. Heinz, J.-F. Paquet, and C. Gale, Thermal photons as a quark-gluon plasma thermometer reexamined, *Phys. Rev. C* **89**, 044910 (2014), arXiv:1308.2440 [nucl-th].
- [7] X.-Y. Wu, C. Gale, S. Jeon, J.-F. Paquet, B. Schenke, and C. Shen, Electromagnetic Radiation from Baryon-Rich Matter in Heavy-Ion Collisions, arXiv:2511.08773 [nucl-th] (2025).
- [8] R. Baier, H. Nakagawa, A. Niegawa, and K. Redlich, Production rate of hard thermal photons and screening of quark mass singularity, *Z. Phys. C* **53**, 433 (1992).

- [9] J. I. Kapusta, P. Lichard, and D. Seibert, High-energy photons from quark - gluon plasma versus hot hadronic gas, *Phys. Rev. D* **44**, 2774 (1991), [Erratum: *Phys. Rev. D* **47**, 4171 (1993)].
- [10] C. M. Hung and E. V. Shuryak, Dilepton / photon production in heavy ion collisions, and the QCD phase transition, *Phys. Rev. C* **56**, 453 (1997), arXiv:hep-ph/9608299.
- [11] J. V. Steele, H. Yamagishi, and I. Zahed, Dilepton and photon emission rates from a hadronic gas, *Phys. Lett. B* **384**, 255 (1996), arXiv:hep-ph/9603290.
- [12] K. Dusling and I. Zahed, Thermal photons from heavy ion collisions: A spectral function approach, *Phys. Rev. C* **82**, 054909 (2010), arXiv:0911.2426 [nucl-th].
- [13] C. H. Lee, J. Wirstam, I. Zahed, and T. H. Hansson, Thermal dileptons from a nonperturbative quark - gluon phase, *Phys. Lett. B* **448**, 168 (1999), arXiv:hep-ph/9809440.
- [14] P. Aurenche, F. Gelis, and H. Zaraket, Landau-Pomeranchuk-Migdal effect in thermal field theory, *Phys. Rev. D* **62**, 096012 (2000), arXiv:hep-ph/0003326.
- [15] T. Peitzmann and M. H. Thoma, Direct photons from relativistic heavy ion collisions, *Phys. Rept.* **364**, 175 (2002), arXiv:hep-ph/0111114.
- [16] S. Turbide, R. Rapp, and C. Gale, Hadronic production of thermal photons, *Phys. Rev. C* **69**, 014903 (2004), arXiv:hep-ph/0308085.
- [17] E. L. Bratkovskaya, S. M. Kiselev, and G. B. Sharkov, Direct photon production from hadronic sources in high-energy heavy-ion collisions, *Phys. Rev. C* **78**, 034905 (2008), arXiv:0806.3465 [nucl-th].
- [18] I. Vitev and B.-W. Zhang, A Systematic study of direct photon production in heavy ion collisions, *Phys. Lett. B* **669**, 337 (2008), arXiv:0804.3805 [hep-ph].
- [19] O. Linnyk, V. Konchakovski, T. Steinert, W. Cassing, and E. L. Bratkovskaya, Hadronic and partonic sources of direct photons in relativistic heavy-ion collisions, *Phys. Rev. C* **92**, 054914 (2015), arXiv:1504.05699 [nucl-th].
- [20] M. Chiu, T. K. Hemmick, V. Khachatryan, A. Leonidov, J. Liao, and L. McLerran, Production of Photons and Dileptons in the Glasma, *Nucl. Phys. A* **900**, 16 (2013), arXiv:1202.3679 [nucl-th].
- [21] L. McLerran and B. Schenke, The Glasma, Photons and the Implications of Anisotropy, *Nucl. Phys. A* **929**, 71 (2014), arXiv:1403.7462 [hep-ph].
- [22] G. Basar, D. Kharzeev, D. Kharzeev, and V. Skokov, Conformal anomaly as a source of soft photons in heavy ion collisions, *Phys. Rev. Lett.* **109**, 202303 (2012), arXiv:1206.1334 [hep-ph].
- [23] K. Tuchin, Electromagnetic radiation by quark-gluon plasma in a magnetic field, *Phys. Rev. C* **87**, 024912 (2013), arXiv:1206.0485 [hep-ph].
- [24] H.-U. Yee, Flows and polarization of early photons with magnetic field at strong coupling, *Phys. Rev. D* **88**, 026001 (2013), arXiv:1303.3571 [nucl-th].
- [25] K. Fukushima and K. Mameda, Wess-Zumino-Witten action and photons from the Chiral Magnetic Effect, *Phys. Rev. D* **86**, 071501 (2012), arXiv:1206.3128 [hep-ph].
- [26] K. A. Mamo and H.-U. Yee, Spin polarized photons and dileptons from axially charged plasma, *Phys. Rev. D* **88**, 114029 (2013), arXiv:1307.8099 [nucl-th].

- [27] K. A. Mamo and H.-U. Yee, Spin polarized photons from an axially charged plasma at weak coupling: Complete leading order, *Phys. Rev. D* **93**, 065053 (2016), arXiv:1512.01316 [hep-ph].
- [28] K. Tuchin, Polarized electromagnetic radiation by chiral media with time-dependent chiral chemical potential, *Phys. Lett. B* **872**, 140080 (2026), arXiv:2508.12923 [hep-ph].
- [29] K. Tuchin, Chiral Cherenkov radiation in the presence of a time-dependent chiral chemical potential, *Phys. Rev. C* **112**, 044903 (2025), arXiv:2507.07324 [hep-ph].
- [30] M. Buzzegoli and K. Tuchin, Electromagnetic radiation at extreme angular velocity, *JHEP* **12**, 113, arXiv:2308.10349 [hep-ph].
- [31] M. Buzzegoli, J. D. Kroth, K. Tuchin, and N. Vijayakumar, Synchrotron radiation by slowly rotating fermions, *Phys. Rev. D* **107**, L051901 (2023), arXiv:2209.02597 [hep-ph].
- [32] M. Buzzegoli, K. Tuchin, and N. Vijayakumar, Quasiclassical approximation of electromagnetic radiation by fermions embedded in a rigidly rotating medium in a strong magnetic field, *Phys. Rev. C* **111**, 054907 (2025), arXiv:2503.06649 [hep-ph].
- [33] J. D. Kroth and K. Tuchin, Sokolov-Ternov effect in rotating systems, *Phys. Rev. D* **111**, 056004 (2025), arXiv:2409.20569 [hep-ph].
- [34] M. Buzzegoli, J. D. Kroth, K. Tuchin, and N. Vijayakumar, Photon radiation by relatively slowly rotating fermions in magnetic field, *Phys. Rev. D* **108**, 096014 (2023), arXiv:2306.03863 [hep-ph].
- [35] D. E. Kharzeev and F. Loschaj, Anomalous soft photon production from the induced currents in Dirac sea, *Phys. Rev. D* **89**, 074053 (2014), arXiv:1308.2716 [hep-ph].
- [36] K. Tuchin, Photon radiation in hot nuclear matter by means of chiral anomalies, *Phys. Rev. C* **99**, 064907 (2019), arXiv:1903.02629 [hep-ph].
- [37] M. Jia, H. Li, and D. Hou, The photon production and collective flows from magnetic induced gluon fusion and splitting in early stage of high energy nuclear collision, *Phys. Lett. B* **846**, 138239 (2023), arXiv:2211.16770 [hep-ph].
- [38] M. Jia, Photon production by chiral magnetic effect in the early stage of high-energy nuclear collisions, *Phys. Rev. D* **111**, 076015 (2025), arXiv:2412.17567 [hep-ph].
- [39] D. Colladay and V. A. Kostelecky, CPT violation and the standard model, *Phys. Rev. D* **55**, 6760 (1997), arXiv:hep-ph/9703464.
- [40] V. A. Kostelecky and A. G. M. Pickering, Vacuum photon splitting in Lorentz violating quantum electrodynamics, *Phys. Rev. Lett.* **91**, 031801 (2003), arXiv:hep-ph/0212382.
- [41] D. E. Kharzeev, L. D. McLerran, and H. J. Warringa, The Effects of topological charge change in heavy ion collisions: 'Event by event P and CP violation', *Nucl. Phys. A* **803**, 227 (2008), arXiv:0711.0950 [hep-ph].
- [42] P. O. Sukhachov, V. A. Miransky, I. A. Shovkovy, and E. V. Gorbar, Collective excitations in Weyl semimetals in the hydrodynamic regime, *J. Phys. Condens. Matter* **30**, 275601 (2018), arXiv:1802.10110 [cond-mat.str-el].

- [43] X.-l. Sheng, D. H. Rischke, D. Vasak, and Q. Wang, Wigner functions for fermions in strong magnetic fields, *Eur. Phys. J. A* **54**, 21 (2018), arXiv:1707.01388 [hep-ph].
- [44] V. Alan Kostelecký, R. Lehnert, M. Schreck, and B. Seradjeh, Nonperturbative Lorentz violation and field quantization, *Phys. Lett. B* **865**, 139414 (2025), arXiv:2412.19733 [hep-th].
- [45] Z. Qiu, G. Cao, and X.-G. Huang, On electrodynamics of chiral matter, *Phys. Rev. D* **95**, 036002 (2017), arXiv:1612.06364 [cond-mat.mes-hall].
- [46] J. Hansen and K. Tuchin, Bremsstrahlung in chiral medium: Anomalous magnetic contribution to the Bethe-Heitler formula, *Phys. Rev. D* **105**, 116008 (2022), arXiv:2203.13134 [hep-ph].
- [47] J. Hansen and K. Tuchin, Electromagnetic bremsstrahlung and energy loss in chiral medium, *Phys. Rev. D* **108**, 076007 (2023), arXiv:2307.05761 [hep-ph].
- [48] J. Hansen and K. Tuchin, Time evolution of parity-odd cascades in homogeneous Abelian and non-Abelian media with chiral imbalance, *Phys. Rev. D* **112**, 014010 (2025), arXiv:2503.00933 [hep-ph].
- [49] J. Hansen, K. Ikeda, D. E. Kharzeev, Q. Li, and K. Tuchin, Magnetic Weyl semimetals as a source of circularly polarized THz radiation, *Phys. Open* **23**, 100268 (2025), arXiv:2405.11076 [cond-mat.mtrl-sci].
- [50] K. Tuchin, Electromagnetic fields in high energy heavy-ion collisions, *Int. J. Mod. Phys. E* **23**, 1430001 (2014).
- [51] K. Tuchin, Excitation of Chandrasekhar-Kendall photons in quark gluon plasma by propagating ultra-relativistic quarks, *Phys. Rev. C* **93**, 054903 (2016), arXiv:1601.05399 [hep-ph].
- [52] K. Tuchin, Radiative instability of quantum electrodynamics in chiral matter, *Phys. Lett. B* **786**, 249 (2018), arXiv:1806.07340 [hep-ph].
- [53] X. Wang and I. A. Shovkovy, Circularly polarized photon emission from magnetized chiral plasmas, *Phys. Rev. D* **110**, 116005 (2024), arXiv:2407.06271 [hep-ph].
- [54] A. Sokolov, I. Ternov, and C. Kilmister, *Radiation from Relativistic Electrons*, American Institute of Physics translation series (American Inst. of Physics, 1986).
- [55] K. S. Kölbig and H. Scherb, On a Hankel transform integral containing an exponential function and two Laguerre polynomials, *Journal of Computational and Applied Mathematics* **71**, 357 (1996).
- [56] K. Mameda, *Chiral symmetry and vacuum structure in rotating relativistic systems*, Ph.D. thesis, The University of Tokyo (2017).
- [57] A. Adare *et al.* (PHENIX), Centrality dependence of low-momentum direct-photon production in Au+Au collisions at $\sqrt{s_{NN}} = 200$ GeV, *Phys. Rev. C* **91**, 064904 (2015), arXiv:1405.3940 [nucl-ex].
- [58] N. J. Abdulameer *et al.* (PHENIX), Nonprompt direct-photon production in Au+Au collisions at $s_{NN}=200$ GeV, *Phys. Rev. C* **109**, 044912 (2024), arXiv:2203.17187 [nucl-ex].
- [59] A. Adare *et al.* (PHENIX), Azimuthally anisotropic emission of low-momentum direct photons in Au+Au collisions at $\sqrt{s_{NN}} = 200$ GeV, *Phys. Rev. C* **94**, 064901 (2016), arXiv:1509.07758 [nucl-ex].
- [60] N. J. Abdulameer *et al.* (PHENIX), Azimuthal anisotropy of direct photons in Au+Au collisions at $\sqrt{s_{NN}} = 200$ GeV, arXiv:2504.02955 [nucl-ex] (2025).

- [61] S. Lin, L. Yan, and Z.-T. Liang, Axial charge fluctuations and chiral magnetic effect in heavy ion collisions, *Phys. Rev. C* **98**, 014903 (2018), arXiv:1802.04941 [nucl-th].
- [62] J. K. Ghosh, S. Grieninger, K. Landsteiner, and S. Morales-Tejera, Is the chiral magnetic effect fast enough?, *Phys. Rev. D* **104**, 046009 (2021), arXiv:2105.05855 [hep-ph].
- [63] K. Fukushima, M. Ruggieri, and R. Gatto, Chiral magnetic effect in the PNJL model, *Phys. Rev. D* **81**, 114031 (2010), arXiv:1003.0047 [hep-ph].
- [64] V. Kovalenko, Evolution and fluctuations of chiral chemical potential in heavy ion collisions, *Int. J. Mod. Phys. E* **33**, 2450037 (2024), arXiv:2312.05155 [hep-ph].
- [65] R. Chatterjee, H. Holopainen, I. Helenius, T. Renk, and K. J. Eskola, Elliptic flow of thermal photons from event-by-event hydrodynamic model, *Phys. Rev. C* **88**, 034901 (2013), arXiv:1305.6443 [hep-ph].
- [66] O. Linnyk, W. Cassing, and E. L. Bratkovskaya, Centrality dependence of the direct photon yield and elliptic flow in heavy-ion collisions at $\sqrt{s_{NN}} = 200$ GeV, *Phys. Rev. C* **89**, 034908 (2014), arXiv:1311.0279 [nucl-th].
- [67] C. Gale, Y. Hidaka, S. Jeon, S. Lin, J.-F. Paquet, R. D. Pisarski, D. Satow, V. V. Skokov, and G. Vujanovic, Production and Elliptic Flow of Dileptons and Photons in a Matrix Model of the Quark-Gluon Plasma, *Phys. Rev. Lett.* **114**, 072301 (2015), arXiv:1409.4778 [hep-ph].
- [68] R. Rapp and H. van Hees, Thermal Electromagnetic Radiation in Heavy-Ion Collisions, *Eur. Phys. J. A* **52**, 257 (2016), arXiv:1608.05279 [hep-ph].
- [69] K. Fukushima, D. E. Kharzeev, and H. J. Warringa, The Chiral Magnetic Effect, *Phys. Rev. D* **78**, 074033 (2008), arXiv:0808.3382 [hep-ph].